Carbon-13 Kinetic Isotope Effects in the Catalytic Oxidation of Carbon Monoxide Over Pd/Al_2O_3

Nives Ogrinc,* Ivan Kobal, and Marjan Senegačnik

J. Stefan Institute, Jamova 39, P.O. Box 3000, 1001 Ljubljana, Slovenia

Received: March 28, 1997[⊗]

The C-13 kinetic isotope effects in the oxidation of CO by oxygen over a 0.5% Pd/γ-Al_2O_3 catalyst were experimentally determined in a temperature range of 323−413 K, and the following temperature dependence was found: $100 \ln(k_{12}/k_{13}) = 3.18-831/T$ (±0.15). A reaction gas mixture of CO/O_2 at a ratio of 1:2 and an initial pressure in a static system ranging from 5 to 10 kPa were used. The reaction kinetics were found to be of order +1 in CO, order 0 in oxygen, and order −1 in CO_2. Under these experimental conditions, an activation energy of 56 ± 3 kJ mol^{-1} was obtained. Using Bigeleisen's formalism based on the absolute rate theory of chemical reactions, kinetic isotope effects were calculated. For the transition state of the rate-determining step, a $(CO_2)^{‡}$ of various geometries and force constants was considered. The experimental data can be satisfactorily interpreted only with an interbond angle close to 110° and a reaction coordinate described by an asymmetric normal vibration of an asymmetric transition state.

1. Introduction

The catalytic oxidation of carbon monoxide is a favorite reaction for a large number of investigators. It is important in locomotive and industrial pollution control.[1] The removal of CO from car exhaust is accomplished by devices using supported Pt, Pd, and Rh catalysts. The content of CO, nitrogen oxides, and hydrocarbons in the exhaust can be reduced by applying three-way catalysts.[2−4] Neither is CO desirable in electric fuel cells, and its content should be addicuously controlled.[5−7] In sealed CO_2 lasers the CO oxidation is carried out in order to recombine CO and O_2 formed by the dissociation of CO_2 in the laser discharge zone.[8] For that purpose so-called NMRO (*noble-metal-reducible-oxide*) catalysts are mainly used. These materials may also be used in CO gas sensors.[9]

In addition to its technological importance, catalytic CO oxidation is also interesting from a theoretical point of view. The participating molecules in the oxidation contain only a few atoms each, and the surface species formed during the reaction is expected to be relatively simple. It is thus assumed that the reaction mechanism will be understood in some detail. This reaction is thus an excellent model reaction for other catalytic systems. Among other catalysts for CO oxidation, well-defined single crystalline as well as polycrystalline Pd surfaces (foils or supported on oxides or metals) have been very frequently investigated.[10] Despite some indications of an Eley-Rideal mechanism,[11−14] it has been widey accepted that the oxidation proceeds via the Langmuir−Hinshelwood reaction between the adsorbed CO and adsorbed O atoms.[10,12,15−32]

The adsorption of CO to the Pd surfaces has been studied through the application of numerous complementary methods. Only the findings essential for our work are summarized below. CO mainly adsorbs undissociatively,[10,15,16,33] although there is an evidence for dissociative adsorption on small Pd particles (edge atoms).[34−36] A small amount of CO may also diffuse into substrate.[34,36−38] The bond between CO and Pd is formed by a mutual donation of electrons from the 5σ orbital of CO into Pd, and back-donation of electrons from the 5d Pd orbitals into the CO 2π* antibonding orbitals.[10,39−50] The CO molecule is thus attached to the surface by its C atom, the CO axis being mostly perpendicular to the surface, or slightly tilted.[22,48,51] The possibility of adsorbing via O atom or by CO lying parallel to the surface may be excluded.[39,45] At small coverages CO molecules are randomly distributed over the metal surface. Further adsorption forces them to arrange into regular layers that get compressed at high coverages[10,15,16,52−55] with the appearance of domain walls[56] and show a tendency for the formation of a close-packed layer with a saturation density that is nearly unaffected by the nature of the substrate surface and its crystallographic orientation.[15,18] Depending on conditions, a CO molecule may be attached to one, two, or three Pd atoms,[18,25,31,40,52,54,55,57−61] which has also been supported by *ab initio* quantum chemical calculations.[43−46,49,62] The adsorption energy depends slightly on the crystal planes[12,18,54,63−65] as well as on the CO coverage—it is lower at high coverages due to the repulsion among adsorbed CO molecules.[10,21,34,39,52,66,67] Smaller Pd supported particles (smaller than 5 nm) produce higher CO binding sites, which may be explained by the high participation of edge sites on smaller particles compared with larger ones.[34] Bridged adsorbed species are more firmly bound than uppermost ones.[31,39,45−47] The adsorption of CO may also induce reconstruction of the Pd surface.[61,68−70]

Adsorption of oxygen to the Pd surface has also been intensively studied using a wide variety of techniques. In summarizing the results we may conclude that oxygen adsorbs molecularly at low temperatures (150 to 200 K) and dissociatively at higher temperatures.[15,18,71−78] It also diffuses into metal producing subsurface oxides[10,15,18,23,74,77,79,80] and may also be dissolved in palladium bulk.[31,81] As with the CO, at small coverage the adsorbed O atoms are distributed randomly over the Pd surface. With increasing coverage the adsorbed species form regular layers that are compressed at higher coverage.[15,72,81,82] In addition to temperature, the borders between different adsorption mechanisms also depend on oxygen coverage.[83−85] Adsorption may also induce reconstruction of the metal surface.[76,83]

In contrast to CO and oxygen, adsorption of CO_2 is very weak; it is impossible to get any measurable amounts of this molecule adsorbed to the surface.[15,18]

[⊗] Abstract published in *Advance ACS Abstracts,* August 15, 1997.

S1089-5639(97)01118-3 CCC: $14.00

Bearing in mind the characteristics of adsorbed CO and oxygen separately, we shall now explain their coadsorption patterns and interactions resulting in surface reactions. Preadsorbed CO inhibits the dissociative chemisorption of oxygen, while the adsorbed O atoms only slightly affect[86] or do not at all affect the possibility for additional uptake of CO.[10,15,16,18,20,22,78,85,87] As is evident from our experimental conditions below, we are primarily interested in the coadsorption when CO and oxygen are admitted to the surface at the same moment. At lower coverages during the coadsorption the adsorbed species of both reactants are distributed randomly over the solid surface.[68,88] As the coverage increases, adsorbed CO and oxygen atoms form ordered isolated domains or islands.[10,15,16,20,22,25,30,64,85,87,89,90] Because of such complex coadsorption patterns, the chemical kinetics of the CO oxidation can not be expected to be very simple. Even though in the majority of investigations reaction orders of about +1 and −1 were found for oxygen and carbon monoxide respectively, these orders substantially depended on the experimental conditions, mainly on temperature, CO and oxygen coverage, and the O_2:CO pressure ratio. They may have zero or even the opposite values with respect to the above ones.[13,16,21,25,31,91] The reaction is always zero order with respect to CO_2. The activation energy of the oxidation depends on the temperature: it is around 50 kJ mol^{-1} at temperatures less than 400 K and around 100 kJ mol^{-1} above.[10,12,15,16,31,91,92] It falls with increasing oxygen coverage: if it is about 100 kJ mol^{-1} at high coverage, it falls to about 50 kJ mol^{-1} at low coverage.[28] It also depends on the particle size: if it is 32 kJ mol^{-1} for 27 nm Pd supported particles, it falls to 19 kJ mol^{-1} for 2.5 nm particles.[93] As on Pt, also on Pd under some specific circumstances the reaction turns to oscillation mode.[21,23,24,26,29,30,61,94−99] Unlike with Pt, here the phenomenon may be explained by the formation of subsurface oxygen or oxygen oxide,[23,24,26] the formation of two-dimensional transition in chemisorbed phase,[96] or a combination of both.[97] Nevertheless, this explanation has not been fully proven.[29] In connection with our work it should also be mentioned that under the steady state conditions, the kinetics of CO oxidation are practically independent of the surface orientation of Pd catalysts.[16,25,54,58,68] CO oxidation has been studied under very different conditions: low and high presurres (pressure gap), single crystals, polycrystals, and supported metals (material gap). It has been shown that there is no significant material gap and that with caution an extrapolation may be made from low- to high-pressure data.[31] This will allow us to compare our results with the wealth of findings in the literature. The overall CO oxidation over Pd may be written in the following steps:

$$O_{2(g)} \rightarrow 2O_{(a)} \quad (1)$$

$$CO_{(g)} \rightarrow CO_{(a)} \quad (2)$$

$$CO_{(a)} + O_{(a)} \rightarrow CO_{2(a)} \quad (3)$$

$$CO_{2(a)} \rightarrow CO_{2(g)} \quad (4)$$

It is evident from the above coadsorption presentation that the Langmuir assumption of an energetically homogeneous surface is not obeyed and that we can hardly talk about a true Langmuir−Hinschelwood mechanism for reaction step 3 between adsorbed CO and O atoms.[10] The reaction takes place along the boundaries between adsorbed CO and adsorbed O domains,[10,15] so that not all the adsorbed O atoms are reactive but only those close enough to the CO domains.[12,20] Adsorbed CO molecules are much more mobile than adsorbed O atoms and may thus reach the O site by climbing and moving over the Pd surface.[10,16,20] There have been some suggestions for the transition state of the reaction 3 above.[18,31,89,90,100−102] The most valuable information about the reaction site and thus about the transition state comes from angular distribution and velocity distribution studies of the desorbing CO_2 formed during the reaction[20,89,90,103−105] and from infrared studies of CO_2 formed.[106,107] The transition state may be a linear,[89,104] but more probably a bent, CO_2.[18,31,85,100,101] Neither CO−Pd−O possibility should be excluded.[25,31,87] The aim of our work was to get additional information on the transition state by studying carbon-13 kinetic isotope effects.

2. Experimental Work

Equipment, Materials, Procedure. All the experiments were carried out in a Pyrex glass vacuum system described elsewhere.[110] Its main parts are 10 dm^3 vessels for storing CO, oxygen, and CO/O_2 mixtures, traps for purification of CO_2, a mercury manometer, a Toepler mercury pump, and a 220 cm^3 cylindrical quartz reaction vessel (∅ 40 mm). The desired reaction temperature was provided by an electric tube kanthal furnace and controlled within ±1 K by means of a thermoregulator connected with a NiCr−Ni thermocouple attached to the outer surface of the reaction vessel. A commercial Pd catalyst was taken: ∅ 6 mm × 3 mm pallets of 0.5% Pd on a γ-Al_2O_3 support, produced by Baker, batch No.3107. Before use the catalysts was outgassed and conditioned for 1 h in hydrogen gas at 40 kPa and a temperature of 573 K. A 99.9% CO, produced by L'Air Liquide, Paris, France, was used without any purification. A commercial oxygen, produced by Ruše, Slovenia, was distilled at liquid nitrogen temperature, and the medium fraction was retained. The main impurity, as determined by mass spectrometry, was nitrogen, below 0.2%. Both gases were mixed to obtain a reaction mixture with a CO/O_2 ratio of 1:2.

3. Reaction Kinetics

The kinetics were studied at temperatures of 323 and 373 K and with 0.56 and 1 g of catalyst. For that purpose, the reaction vessel was connected to a mercury manometer and the total pressure was followed during the reaction. Two typical pressure runs are shown in Figure 1. The following two kinetic laws were tested

$$-\frac{dP_{CO}}{dt} = k\frac{P_{O_2}}{P_{CO}} = k\frac{P_t - 2(P_0 - P_\infty)}{2(P_t - P_\infty)} \quad (5)$$

$$-\frac{dP_{CO}}{dt} = k\frac{P_{CO}}{P_{CO_2}} = k\frac{P_t - P_\infty}{P_0 - P_t} \quad (6)$$

in which the partial pressures are expressed via the total pressure according to the following relations

$$P_{CO} = 2(P_t - P_\infty) \quad (7)$$

$$P_{O_2} = P_t - 2(P_0 - P_\infty) \quad (8)$$

$$P_{CO_2} = 2(P_0 - P_t) \quad (9)$$

P_0, P_t, and P_∞ being the total pressures at times 0, t, and ∞.

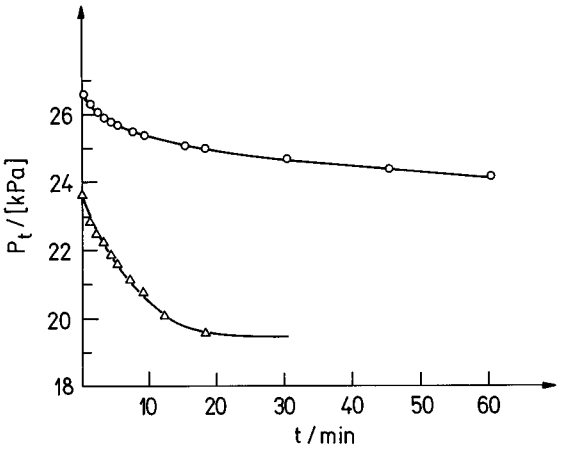

Figure 1. Two examples of the P_t total pressure runs in the catalytic oxidation of CO over a Pd/Al_2O_3 catalyst: (○) 323 K ($P_0 = 26.6$ kPa, $P_\infty = 22.5$ kPa); (△) 373 K ($P_0 = 23.7$ kPa, $P_\infty = 19.8$ kPa).

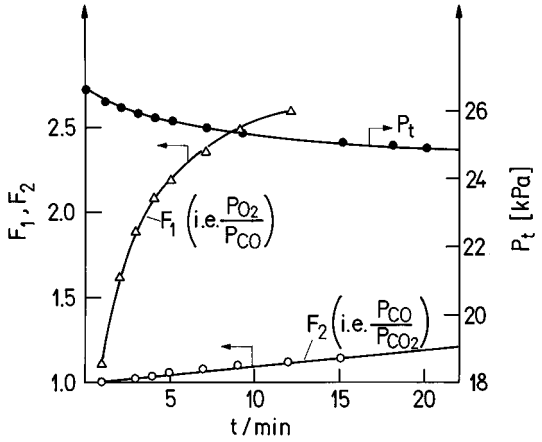

Figure 2. Checking the experimental data for the kinetic laws $F_1(P_0, P_t, P_\infty)$ (△), eq 10, and $F_2(P_0, P_t, P_\infty)$ (○), eq 11; (●) P_t ($P_0 = 26.6$ kPa, $P_\infty = 22.5$ kPa).

The above kinetic equations become after integration respectively

$$F_1 = (P_0 - P_t) + [P_\infty - 2(P_0 - P_\infty)] \ln\frac{P_t - 2(P_0 - P_\infty)}{P_0 - 2(P_0 - P_\infty)} = F_1(P_0, P_t, P_\infty) = \frac{1}{4}kt \quad (10)$$

$$F_2 = (P_0 - P_\infty) \ln\frac{P_0 - P_\infty}{P_t - P_\infty} - (P_0 - P_t) = F_2(P_0, P_t, P_\infty) = \frac{1}{2}kt \quad (11)$$

When the experimental data are input into the above expressions, only F_2 gives a straight line, as shown in Figure 2. This is also confirmed by Figure 3 for two masses of catalyst. Thus we may conclude that under our experimental conditions, the reaction orders are +1 for CO, −1 for CO_2, and 0 for O_2. It is well-known that CO_2 desorbes immediately after being formed;[15,18] thus, the inhibition of CO_2 found in our steady state experiments may be explained by a readsorption of CO_2. Another explanation would be the formation of carbon on the surface followed by a decrease of reaction rate,[34,35,37,108,109] which could then be manifested as a CO_2 inhibition.

In order to enable a comparison of reaction rates for different masses of catalyst, the following relation is useful

$$k = k_{abs}\frac{m}{V} \quad (12)$$

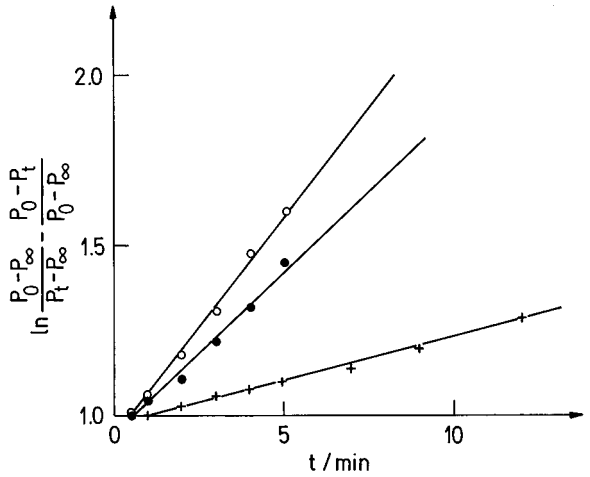

Figure 3. Reaction kinetics for various masses of catalyst at 373 K: (+) 0.56 g ($P_0 = 24.1$ kPa, $P_\infty = 20.3$ kPa); (○) 1 g ($P_0 = 22.9$ kPa, $P_\infty = 19.3$ kPa); (●) 1 g ($P_0 = 22.6$ kPa, $P_\infty = 19.1$ kPa).

in which k_{abs} stands for the absolute rate constant reduced to the mass of catalyst, m, and the reaction volume, V.

If in expression 6 the differences of the total pressures are expressed by P^0_{CO} (the initial CO partial pressure), P_∞, and the extent of reaction, f, reached within a time t, then we may write

$$k_{abs} = \frac{V}{tm}P^0_{CO}\left(\ln\frac{1}{1-f} - f\right) \quad (13)$$

4. Kinetic Isotope Effects

At least these two isotopic reactions run simultaneously in the catalytic oxidation of carbon monoxide of a natural isotopic composition

$$^{12}CO + {}^1/_2O_2 \xrightarrow{k_{12}} {}^{12}CO_2$$

$$^{13}CO + {}^1/_2O_2 \xrightarrow{k_{13}} {}^{13}CO_2 \quad (14)$$

and the carbon-13 kinetic isotope effect (KIE-13) may be defined as follows

$$\text{KIE-13} = 100 \ln(k_{12}/k_{13}) \quad (15)$$

For the measurement of the kinetic isotope effects, the reaction vessel with the catalyst was heated to a desired temperature, the reactant gas mixture was added, and the reaction was allowed to run up to a desired extent of reaction. Carbon dioxide formed was isolated in a trap cooled with liquid nitrogen by means of the Toepler pump and then further purified by several distillations between two traps cooled with liquid nitrogen (77 K) and a mixture of CCl_4-CHCl_2-liquid nitrogen (195 K) respectively. The kinetic isotope effects were calculated via the equation[111]

$$\frac{k_{12}}{k_{13}} = \frac{\ln(1-f)}{\ln\left(1 - f\cdot S\binom{13}{12}\right)} \quad (16)$$

where $S\binom{13}{12}$ stands for the C-13 isotopic enrichment of the CO_2

TABLE 1: Experimental Conditions and Experimental Results of the C-13 Kinetic Isotope Determination in the Oxidation of CO over Pd/Al_2O_3 Catalyst

T, K	catalyst mass, mg	P^0_{CO}, kPa	t, min	f	$S(^{13}_{12})$	$100 \times \ln(k_{12}/k_{13})$	$10^3\, k_{abs}$, $m^2\ s^{-3}$
323	560	7.98	90	0.1038	0.9931	0.73	3.3
		9.87	95	0.1072	0.9938	0.67	4.3
		8.70	90	0.1173	0.9940	0.65	4.6
		8.70	90	0.1249	0.9937	0.68	5.3
353	560	8.26	8	0.0670	0.9922	0.81	15.4
		8.81	10	0.0780	0.9905	1.00	18.4
		8.30	12	0.1095	0.9890	1.16	28.6
		5.91	15	0.1668	0.9915	0.95	40.0
		8.35	7	0.1200	0.9943	0.61	59.3
383	80	9.67	40	0.1370	0.9910	0.97	113
		9.99	35	0.1360	0.9912	0.96	130
		10.08	30	0.1180	0.9912	0.95	114
		9.74	35	0.1345	0.9913	0.95	125
		10.31	30	0.1130	0.9912	0.95	105
		9.75	39	0.1340	0.9915	0.93	112
413	40	9.26	6	0.0770	0.9867	1.39	434
		9.34	15	0.1410	0.9866	1.45	617
		8.88	10	0.0790	0.9896	1.08	264
		8.95	10	0.0860	0.9877	1.29	314

formed up to an extent of reaction f and is defined by

$$S\left(\frac{13}{12}\right) = \frac{\dfrac{[^{13}C^{16}O_2]_f}{[^{12}C^{16}O_2]_f}}{\dfrac{[^{13}C^{16}O_2]_1}{[^{12}C^{16}O_2]_1}} \tag{17}$$

and obtained by analyzing the CO_2 at the extent of reaction $f = f$ and $f = 1$ (CO_2 at $f = 1$ has the same isotopic composition as the unreacted CO), respectively, on a double-collector mass spectrometer.[112]

In Table 1 the main experimental data are collected. The temperature dependence of the kinetic isotope effects may be expressed by

$$100 \ln\left(\frac{k_{12}}{k_{13}}\right) = 3.18 - \frac{831}{T}\ (\pm 0.15) \tag{18}$$

If the k_{abs} values from Table 1, as calculated by using eq 13, are plotted in the Arrhenius diagram, Figure 4 is obtained resulting in an activation energy of 56 ± 3 kJ mol^{-1}.

5. Discussion

Theoretical interpretation of the experimental kinetic isotope effects was made following Bigeleisen's formalism[113,114] based on the absolute rate theory. The carbon-13 kinetic isotope effects may accordingly be calculated[114] from the equation

$$\frac{k_1}{k_2} = \frac{\nu^{\ddagger}_{L1}}{\nu^{\ddagger}_{L2}} \prod_{i=1}^{3n-6} \frac{u_{2i}\sinh(u_{1i}/2)}{u_{1i}\sinh(u_{2i}/2)} \prod_{i=1}^{3n^{\ddagger}-7} \frac{u^{\ddagger}_{1i}}{u^{\ddagger}_{2i}} \frac{\sinh(u^{\ddagger}_{2i}/2)}{\sinh(u^{\ddagger}_{1i}/2)} \tag{19}$$

in which ‡ denotes the transition state. The first product runs over all the isotopic frequencies of the reactant and the second one over the real frequencies of the transition state, ν_L is the frequency belonging to the reaction coordinate, $\nu = hc\omega/k_BT$ (ω, wavenumber in cm^{-1}; h, Planck's constant; k_B, Boltzmann's constant; c, speed of light; T, temperature).

The isotopic normal frequencies for the reactant CO molecule were obtained from the literature,[115] while those for the transition state were obtained by solving Wilson's FG matrix equation[116,117]

$$\mathbf{GFL} = \mathbf{L\Lambda} \tag{20}$$

in which **G** is the Wilson matrix, **F** is the force-constant matrix, **L** is the eigenvector matrix, and $\mathbf{\Lambda}$ is a diagonal matrix of eigenvalues $\lambda_{ii} = 4\pi^2\nu_i^2$ with ν_i equal to the frequency of the ith normal vibration.

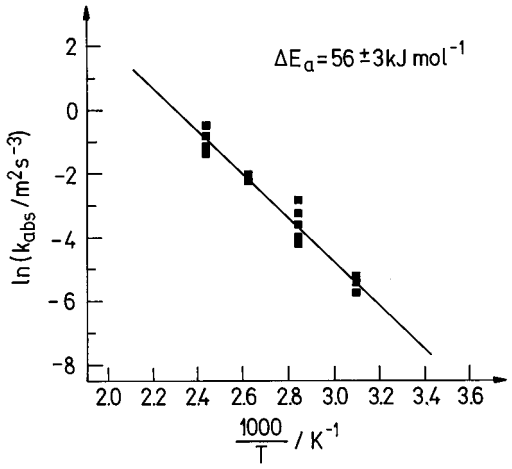

Figure 4. Arrhenius plot of the overall rate constants k_{abs} (eq 13).

For the rate-determining elementary step (eq 3 above) of the reaction mechanism, for which Bigeleisen's formula is valid, a bent $(CO_2)^{\ddagger}$ transition state was supposed. For its internal coordinates, changes of both C−O bond lengths, designated by D and d, and of the interbond angle α were taken. In calculations the values of diagonal **F** matrix elements were varied in the following ranges: F_D and F_d from 100 to 2000 N m^{-1} in steps of 100 N m^{-1}; F_α from 50 to 300 N m^{-1} in steps of 50 N m^{-1} (100 N m^{-1} equals 1 mdyn A^{-1}). The interbond angle α took values between 80 and 170° in 10° steps. The off-diagonal elements were set zero, with the only exception of the F_{Dd} element needed to get a zero determinant of the **F** matrix, thus resulting in one zero normal frequency belonging to the reaction coordinate. Its value was calculated from the equation

$$F_{Dd} = \pm\sqrt{(F_D \cdot F_d)} \tag{21}$$

In our case only an asymmetric stretching vibrational normal mode of the transition state can describe the movement along the reaction coordinate−CO_2 formation: one of the bonds is weakened from its value in CO (2000 N m^{-1})[118,119] to a value in CO_2 (1600 N m^{-1}),[119] while the other bond is formed, thus having a stretching force constant between zero and a value in CO_2. Hence in our calculations the "+" sign was used in the above equation. An agreement between the calculated and experimental kinetic isotope effects was sought by a graphic method already used in the catalytic oxidation of CO over NiO and ZnO,[120,121] in which for selected values of other parameters of the transition state, a region of acceptable values of both stretching force constants (such as giving an agreement with experiment) is plotted. Figure 5 shows two examples of such regions for several values of F_α and interbond angles α of 80° and 90°, respectively. We see that higher interbond angles are accompanied by higher stretching force constants. This is further confirmed in Figure 6 where acceptable regions for 100° and 110° angles are plotted together. As seen in Figure 7, for the 120° angle, acceptable regions were found only for the values of bending force constants being unrealistically high.[122−125]

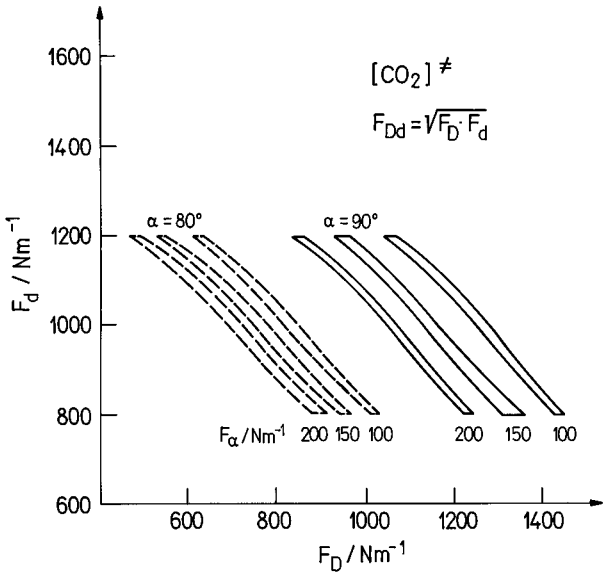

Figure 5. Ranges of acceptable values of both stretching force constants for selected values of the bending force constant and an interbond angle of 80° and 90°.

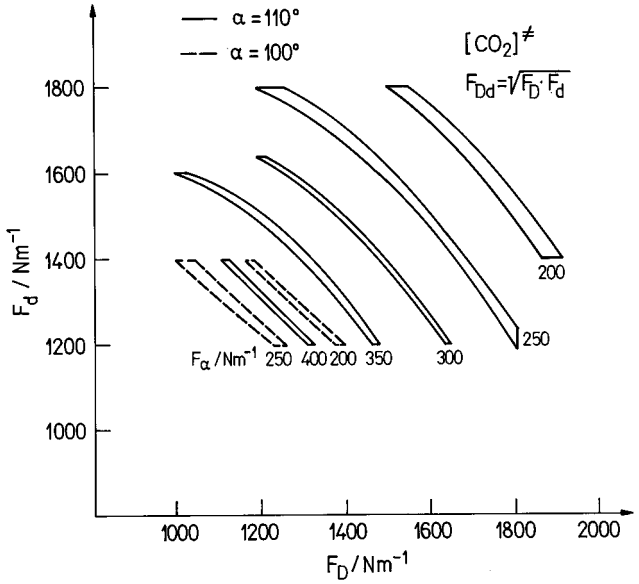

Figure 6. Ranges of acceptable values of both stretching force constants for selected values of the bending force constant and interbond angles of 100° and 110°.

TABLE 2: Geometries, Force Constants, and Isotopic Frequencies of Normal Vibrations of Two Successful Examples of the $(CO_2)^{\ddagger}$ Transition State

	F_D, N m^{-1}	F_d, N m^{-1}	F_α, N m^{-1}	D, nm	d, nm	ω_{12}, cm^{-1}	ω_{13}, cm^{-1}
(1)	1800	1200	250	0.112	0.121	2524.2	2472.5
						853.8	846.4
						0	0
(2)	1600	1200	300	0.115	0.121	2457.8	2406.0
						914.9	907.8
						0	0

For interbond angles above 120° no agreement with experiment can be obtained. Because of the asymmetric motion of the reaction coordinate, in Figures 5−7 only regions with one of the stretching force constants above and the other below 1600 N m^{-1} are of interest. We see that angles α of 100° and below do not fit our requirements. Because no acceptable ranges of parameter values were found for angles α above 110°, only a transition state with an interbond angle around 110° is appropriate. In Figure 8 agreement with experiment is shown for two sets of the transition state parameter values listed in Table 2.

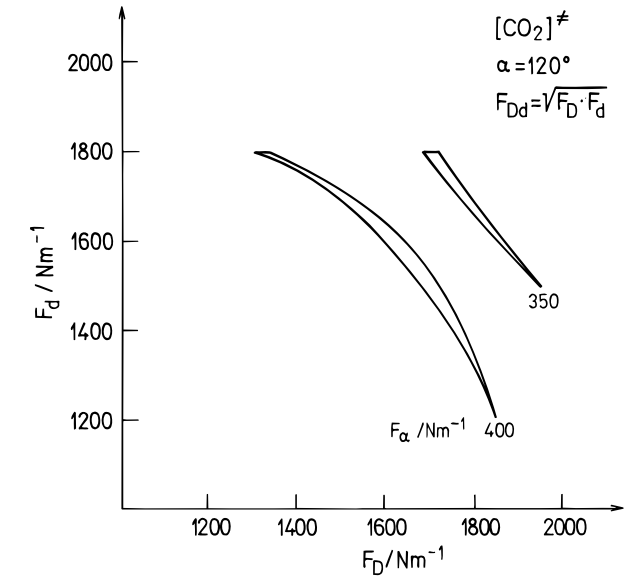

Figure 7. Ranges of acceptable values of both stretching force constants for selected values of the bending force constant and an interbond angle of 120°.

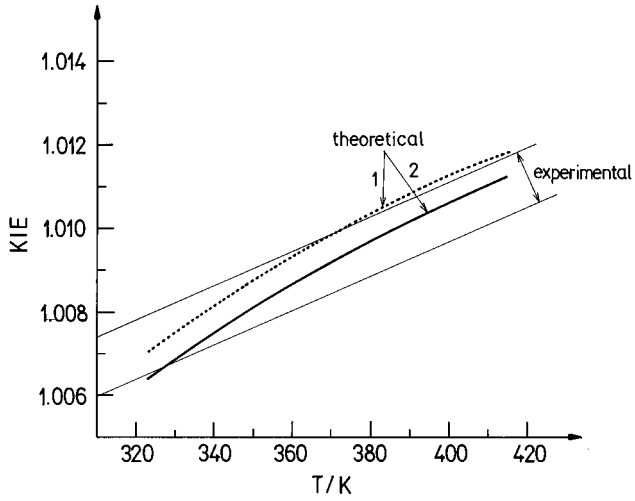

Figure 8. Agreement with the experiment for two successful examples of the $(CO_2)^{\ddagger}$ transition state with parameter values collected under (1) and (2) in Table 2.

6. Conclusions

Our study of the C-13 kinetic isotope effects in the catalytic oxidation of CO over Pd confirms a bent structure of the $(CO_2)^{\ddagger}$ transition state of the rate-determining step of the reaction mechanism of this reaction. Its interbond angle is around 110°, which is close to the structure suggested before on the basis of other experimental data.[85] The reaction coordinate is described by an asymmetric motion of the transition state: one C−O bond is weakened while the other one is being formed. Due to this limitation only an asymmetric transition state is acceptable, even though there are also indications of a symmetric structure.[101] The resulting acceptable values of force constants of the transition state are shown in Figure 8, while in Table 2 values of geometric parameters and isotopic frequencies of normal vibrations for two examples are collected.

Acknowledgment. The authors are greatful to Dr. V. Kramer at the J. Stefan Institute for performing mass-spectrometric

analyses. The work was funded by the Ministry of Science and Technology of the Republic of Slovenia.

References and Notes

(1) Kummer, J. T. *J. Phys. Chem.* **1986**, *90*, 4747.
(2) Kašpar, J.; de Leitenburg, C.; Fornasiero, P.; Trovarelli, A.; Graziani, M. *J. Catal.* **1994**, *146*, 136.
(3) Fornasiero, P.; Di Monte, R.; Ranga Rao, G.; Kašpar, J.; Meriani, S.; Trovarelli, A.; Graziani, M. *J. Catal.* **1995**, *151*, 168.
(4) Ranga Rao, G.; Fornasiero, P.; Di Monte, R.; Kašpar, J.; Vlaic, G.; Balducci, G.; Meriani, S.; Gubitosa, G.; Cremona, A.; Graziani, M. *J. Catal.* **1996**, *162*, 1.
(5) Ianniello, R.; Schmidt, V. M.; Stimming, U.; Stumper, J.; Wallau, A. *Electrochim. Acta* **1994**, *39*, 1863.
(6) Friedrich, K. A.; Geyzers, K. -G.; Linke, U.; Stimming, U.; Stumper, J. *J. Electroanal. Chem.* **1996**, *402*, 123.
(7) Friedrich, K. A.; Linke, U.; Stimming, U.; Stumper, J.; Vogel, R. *1st International Symposium on Proton Conducting Fuel Cells*; Gottesfeld, Ed.; The Electochemical Society Proceedings Series; 1995; PV 95−23, p 299.
(8) Low-Temperature-CO-Oxidation Catalysis for Long-Life CO_2 Lasers. NASA Conference Publication 3076; Schryer, D. R., Hoflund, G. B., Eds.: NASA: Virginia, 1990.
(9) Herz, R. K. In Low-Teperature-CO-Oxidation Catalysis for Long-Life CO_2 Lasers. NASA Conference Publication 3076; Schryer, D. R., Hoflund, G. B., Eds.; NASA: Virginia, 1990; pp 21.
(10) Gasser, R. P. H. *An Introduction to Chemisorption and Catalysis by Metals;* Clarendon Press: Oxford, 1985.
(11) Ertl, G.; Rau, P. *Surf. Sci.* **1969**, *15*, 443.
(12) Matsushima, T.; White, J. M. *J. Catal.* **1975**, *40*, 334.
(13) Matsushima, T.; White, J. M. *Surf. Sci.* **1977**, *67*, 122.
(14) Strozier,Jr., J. A.; Cosgrove, G. J.; Fischer, D. A. *Surf. Sci.* **1979**, *82*, 481.
(15) Conrad, H.; Ertl, G.; Küppers, J. *Surf. Sci.* **1978**, *76*, 323.
(16) Engel, T.; Ertl, G. *J. Chem. Phys.* **1978**, *69*, 1267.
(17) Smolikov, M. D.; Savchenko, V. I. *React. Kinet. Catal. Lett.* **1979**, *12*, 457.
(18) Engel, T.; Ertl, G. In *The Chemical Physics of Solid Surfaces and Heterogeneous Catalysis*; King, D. A., Woodruff, D. P., Eds.; Elsevier: Amsterdam, 1982; Vol 4: *Fundamental Studies of Heterogenous Catalysis*, Chapter 3.
(19) Madix, R. J. In *The Chemical Physics of Solid Surfaces and Heterogeneous Catalysis*; King, D. A., Woodruff, D. P., Eds.; Elsevier: Amsterdam, 1982; Vol 4: *Fundamental Studies of Heterogenous Catalysis*, Chapter 1.
(20) Ohno, Y.; Matsushima, T.; Shobatake, K. *Surf. Sci.* **1992**, *273*, 291.
(21) Berlowitz, P. J.; Peden, C. H. F.; Goodman, D. W. *J. Phys. Chem.* **1988**, *92*, 5213.
(22) Odörfer, G.; Plummer, E. W.; Freund, H. -J.; Kuhlenbeck, H.; Neumann, M. *Surf. Sci.* **1988**, *198*, 331.
(23) Ladas, S.; Imbihl, R.; Ertl, G. *Surf. Sci.* **1989**, *219*, 88.
(24) Bassett, M. R.; Imbihl, R. *J. Chem. Phys.* **1990**, *93*, 1.
(25) Matolin, V.; Gillet, E.; Reed, N. M.; Vickerman, J. C. *J. Chem. Soc., Faraday Trans.* **1990**, *86*, 2749.
(26) Yamamoto, T.; Kasai, H.; Okiji, A. *J. Phys. Soc. Jpn.* **1991**, *60*, 982.
(27) Choi, K. I.; Vannice, M. A. *J. Catal.* **1991**, *131*, 1.
(28) Wada, E.; Funakoshi, J.; Kanemas, S. *J. Chem. Soc. Jpn.* **1992**, *65*, 2456.
(29) Bondzie, V.; Kleban, P; Browne D. A. *J. Vac. Sci. Technol. A* **1993**, *11*, 1946.
(30) Ehsasi, M.; Berdau, M.; Rebitzki, T.; Charlé, K. -P.; Christmann, K.; Block, J. H. *J. Chem. Phys.* **1993**, *98*, 11.
(31) Xu, X.; Goodman, D. W. *J. Phys. Chem.* **1993**, *97*, 7711.
(32) Park, S. -J.; Lee, C. W.; Kim, Y. -S.; Chong, P. J. *Bull. Korean Chem. Soc.* **1995**, *16*, 183.
(33) Matsushima, T. *Surf. Sci.* **1985**, *157*, 297.
(34) Gillet, E.; Channakhone, S.; Matolin, V. *J. Catal.* **1986**, *97*, 437.
(35) Joyal, C. L. M.; Butt, J. B. *J. Chem. Soc., Faraday Trans. 1* **1987**, *83*, 2757.
(36) Henry, C. R. *Surf. Sci.* **1989**, *223*, 519.
(37) Matolin, V.; Rebholz, M.; Kruse, N. *Surf. Sci.* **1991**, *245*, 233.
(38) von Oertzen, A.; Rotermund, H. H.; Nettesheim, S. *Chem. Phys. Lett.* **1992**, *199*, 131.
(39) Tracy, J. C.; Palmberg, P. W. *J. Chem. Phys.* **1969**, *51*, 4852.
(40) March, N. H. In *Physics of Solids and Liquids*: *Chemical Bonds Outside Metal Surfaces*; Devreese, J. T., Evrard, R. P., Lundqvist, S., Mahan, G. D., March, N. H., Eds.; Plenum Press: New York and London, 1982.
(41) Bader, S. D.; Blakely, J. M.; Brodsky, M. B.; Friddle, R. J.; Panosh, R. L. *Surf. Sci.* **1978**, *74*, 405.
(42) Campuzano, J. C. In *The Chemical Physics of Solid Surfaces and Heterogeneous Catalysis*; King, D. A., Woodruff, D. P., Eds.; Elsevier: Amsterdam, 1982; Vol 3: *Chemisorption System*; Chapter 4.
(43) Pacchioni, G.; Bagus, P. S. *J. Chem. Phys.* **1990**, *93*, 1209.
(44) Bagus, P. S.; Pacchioni, G. *Surf. Sci.* **1990**, *236*, 233.
(45) Smith, G. W.; Carter, E. A. *J. Phys. Chem.* **1991**, *95*, 2327.
(46) Björneholm, O.; Nilsson, A.; Zdansky, E. O. F.; Sandell, A.; Hernnäs, B.; Tillborg, H.; Andersen, J. N.; Märtensson, N. *Phys. Rev. B* **1992**, *46* (10), 353.
(47) Volpilhac, G.; Baba, M. F.; Achard, F. *J. Chem. Phys.* **1992**, *97*, 2126.
(48) Bertel, E.; Memmel, N.; Rangelov, G.; Bischler, U. *Chem. Phys.* **1993**, *177*, 337.
(49) Pick, S. *J. Phys. Chem.* **1995**, *99*, 15375.
(50) Schulze Icking-Konert, G.; Handschuh, H.; Ganteför, G.; Eberhardt, W. *Phys. Rev. Lett.* **1996**, *76*, 1047.
(51) Madey, T. E.; Yates, Jr., J. T.; Bradshaw, A. M.; Hoffmann, F. M. *Surf. Sci.* **1979**, *89*, 370.
(52) Behm, R. J.; Christmann, K.; Ertl, G.; Van Hove, M. A. *J. Chem. Phys.* **1980**, *73*, 2984.
(53) Gotoh, Y.; Vook, R. W. *Colloids Surf.* **1989**, *37*, 149.
(54) Szanyi, J.; Kuhn, W. K.; Goodman, D. W. *J. Vac. Sci. Technol.* **1993**, *11*, 1969.
(55) Andersen, J. N.; Qvarford, M.; Nyholm, R.; Sorensen, S. L.; Wigren, C. *Phys. Rev. Lett.* **1991**, *67*, 2822.
(56) Berndt, W.; Bradshaw, A. M. *Surf. Sci. Lett.* **1992**, *279*, L165.
(57) Szilágyi, T.; Sárkány, A.; Mink, J.; Tétényi, P. *Acta Chim. Acad. Sci. Hung., Tomus* **1979**, *100*, 409.
(58) Hendrickx, H. A. C. M.; des Bouvrie, C; Ponec, V. *J. Catal.* **1989**, *115*, 601.
(59) Matolin, V.; Gillet, E.; Channakhone, S., *J. Catal.* **1986**, *97*, 448.
(60) Kruse, N.; Gillet, E. *Z. Phys. D: At., Mol. Clusters* **1989**, *12*, 575.
(61) Raval, R.; Haq, S.; Harrison, M. A.; Blyholder, G.; King, D. A. *Chem. Phys. Lett.* **1990**, *167*, 391.
(62) Pedocchi, L.; Ji, M. R.; Lizzit, S.; Comelli, G.; Rovida, G. *J. Electron Spectrosc. Relat. Phenom.* **1995**, *76*, 383.
(63) Toyoshima, I.; Somorjai, G. A. *Catal. Rev.-Sci. Eng.* **1979**, *19*, 105.
(64) Halsey, G. D. *Surf. Sci.* **1977**, *64*, 681.
(65) Galeev, T. K.; Bulgakov, N. N.; Savelieva, G. A.; Popova, N. M. *React. Kinet. Catal. Lett.* **1980**, *14*, 56.
(66) Gou, X.; Yates, Jr., J. T. *J. Chem. Phys.* **1989**, *90*, 6761.
(67) Guerrero, A.; Reading, M.; Grillet, Y.; Rouquerol, J.; Boitiaux, J. P.; Cosyns, J. *Z. Phys. D: At., Mol. Clusters* **1989**, *12*, 583.
(68) Gaussmann, A.; Kruse, N. *Catal. Lett.* **1991**, *1*, 305.
(69) Gaussmann, A.; Kruse, N. *Surf. Sci.* **1992**, *266*, 46.
(70) Gaussmann, A.; Kruse, N. *Surf. Sci.* **1992**, *279*, 319.
(71) He, J. -W.; Norton, P. R. *Surf. Sci.* **1988**, *204*, 26.
(72) He, J. -W.; Memmert, U.; Griffiths, K.; Norton, P. R. *J. Chem. Phys.* **1989**, *90*, 5082.
(73) He, J. -W.; Memmert, U.; Norton, P. R. *J. Chem. Phys.* **1989**, *90*, 5088.
(74) Guo, X.; Hoffman, A.; Yates, Jr., J. T. *J. Chem. Phys.* **1989**, *90*, 5787.
(75) Milun, M.; Pervan, P.; Vajić, M.; Wandelt, K. *Surf. Sci.* **1989**, *211*, 887.
(76) Simmons, G. W.; Wang, Y. -N.; Marcos, J.; Klier, K. *J. Phys. Chem* **1991**, *95*, 5422.
(77) Hasselbrink, E.; Hirayama, H.; de Meijere, A.; Weik, F.; Wolf, M.; Ertl, G. *Surf. Sci.* **1992**, *269/270*, 235.
(78) Kolasiński, K. W.; Cemi c, F.; de Meijere, A.; Hasselbrink, E. *Surf. Sci.* **1995**, *334*, 19.
(79) Imbihl, R.; Demuth, J. E.; *Surf. Sci.* **1986**, *173*, 395.
(80) Matsushima, T. *Surf. Sci.* **1989**, *217*, 155.
(81) Conrad, H.; Ertl, G.; Küppers, J.; Latta, E. E. *Surf. Sci.* **1977**, *65*, 245.
(82) He, J. -W.; Memmert, U.; Griffiths, K.; Lennard, W. N.; Norton, P. R. *Surf. Sci.* **1988**, *202*, L555.
(83) Klier, K.; Wang, Y. -N.; Simmons, G. W. *J. Phys. Chem.* **1993**, *97*, 633.
(84) Chang, S.-L.; Thiel, P. A. *J. Chem. Phys.* **1988**, *88*, 2071.
(85) Matsushima, T.; Asada, H. *J. Chem. Phys.* **1986**, *85*, 1658.
(86) Goschnick, J.; Grunze, M.; Loboda-Cackovic, J.; Block, J. H. *Surf. Sci.* **1987**, *189/190*, 137.
(87) Stuve, E. M.; Madix, R. J.; Brundle, C. R. *Surf. Sci.* **1981**, *146*, 155.
(88) Matolin, V.; Gillet, E.; Gillet, M. *Surf. Sci.* **1985**, *162*, 345.
(89) Matsushima, T. *J. Chem. Phys.* **1989**, *91*, 5722.
(90) Matsushima, T. *J. Chem. Phys.* **1992**, *97*, 2783.
(91) Szanyi, J.; Goodman, D. W. *J. Phys. Chem.* **1994**, *98*, 2972.
(92) Szanyi, J.; Kuhn, W. K.; Goodman, D. W. *J. Phys. Chem.* **1994**, *98*, 2978.
(93) Stará, I.; Nehasil, V.; Matolín, V. *Surf. Sci.* **1995**, *331−333*, 173.
(94) Plath, P. J.; Möller, K.; Jaeger, N. I. *J. Chem. Soc., Faraday Trans. 1* **1988**, *84*, 1751.
(95) Svensson, P.; Jaeger, N. I.; Plath, P. J. *J. Phys. Chem.* **1988**, *92*, 1882.
(96) Schüth, F.; Wicke, E. *Ber. Bunsen-Ges. Phys. Chem.* **1989**, *93*, 491.

(97) Ehsasi, M.; Seidel, C.; Ruppender, H.; Drachsel, W.; Block, J. H. *Surf. Sci. Lett.* **1989**, *210*, L198.
(98) Ehsasi, M.; Frank, O.; Block, J. H.; Christmann, K. *Chem. Phys. Lett.* **1990**, *165*, 115.
(99) Levine, H.; Zou, X. *J. Chem. Phys.* **1991**, *95*, 3815.
(100) Freund, H. -J.; Messmer, R. P. *Surf. Sci.* **1986**, *172*, 1.
(101) Coulston, G. W.; Haller, G. L. *J. Chem. Phys.* **1991**, *95*, 6932.
(102) Uetsuka, H.; Watanabe, K.; Ohnuma, H.; Kunimori, K. *Chem. Lett., Chem. Soc. Jpn.* **1996**, 227.
(103) Matsushima, T. *Vacuum* **1990**, *41*, 275.
(104) Matsushima, T.; Shobatake, K.; Ohno, Y. *Surf. Sci.* **1993**, *283*, 101.
(105) Matsushima, T.; Shobatake, K.; Ohmo, Y.; Nagai, K.; Tabayashi, K. *Chem. Phys. Lett.* **1991**, *187*, 277.
(106) Watanabe, K.; Uetsuka, H.; Ohnuma, H.; Kunimori, K. *Appl. Surf. Sci.* **1996**, *99*, 411.
(107) Uetsuka, H.; Watanabe, K.; Kunimori, K. *Surf. Sci.* **1996**, *363*, 73.
(108) Tomková, E.; Mašek, K.; Matolin, V. *Z. Phys. D: At., Mol. Clusters* **1988**, *10*, 499.
(109) Graham, G. W.; Logan, A. D.; Shelef, M. *J. Phys. Chem.* **1993**, *97*, 5445.
(110) Kobal. I.; Senegačnik, M.; Kobal H. *J. Catal.* **1977**, *49*, 1.
(111) Senegačnik, M., Ph.D. Thesis, University of Ljubljana, Ljubljana 1971.
(112) Craig, H. *Geochim. Cosmochim. Acta* **1957**, *12*, 133.
(113) Bigeleisen, J.; Goeppert-Mayer, M. *J. Chem. Phys.* **1947**, *15*, 201.
(114) Van Hook, W. A. *Isotope Effects in Chemical Reactions*; Van Nostrand-Reinhold: New York, 1970.
(115) Nakamoto, K. *Infrared Spectra of Inorganic and Coordination Compounds*; Wiley: New York, 1963.
(116) Wilson, E. B.; Decius, J. C.; Cross, P. C. *Molecular Vibrations*; McGraw Hill: New York, 1965.
(117) Guns, P. *Vibrating Molecules*; Chapman & Hall: London, 1971.
(118) Politzer, P.; Kasten, S. D. *Surf. Sci.* **1973**, *36*, 186.
(119) Herzberg, G. *Molecular Spectra and Molecular Structure II, Infrared and Raman Spectra of Polyatomic Molecules*: Van Nostrand: New York, 1949.
(120) Kobal, I.; Senegačnik, M.; Barlič, B. *J. Chem. Phys.* **1978**, *69*, 174.
(121) Kobal, I.; Senegačnik, M.; Kobal, H. *J. Chem. Phys.* **1983**, *78*, 1815.
(122) Pacansky, J.; Wahlgren, U.; Bagus, P. S. *J. Chem. Phys.* **1975**, *62*, 2740.
(123) Cooper, C. D.; Compton, R. N. *J. Chem. Phys.* **1973**, *59*, 3550.
(124) Dalal, N. S.; McDowell, C. A.; Park, J. M. *J. Chem. Phys.* **1975**, *63*, 1856.
(125) Shapira, Y.; Cox, S. M.; Lichtman, D. *Surf. Sci.* **1976**, *54*, 43.